

AD-A147 369

APPLICATION OF THE DIFFRACTION MODEL TO AMORPHOUS  
MAGNESIUM ZINC ALLOYS. (U) ARMY ARMAMENT RESEARCH AND  
DEVELOPMENT CENTER WATERVLIET NY L. P J COTE ET AL.

1/1

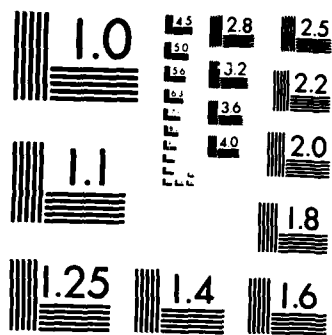
UNCLASSIFIED

SEP 84 ARLCB-TR-84031 SBI-AD-E440 259

F/G 11/6

NL





MICROCOPY RESOLUTION TEST CHART  
NATIONAL BUREAU OF STANDARDS-1963-A

16

AD

TECHNICAL REPORT ARLCB-TR-84031

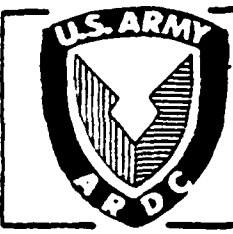
AD-E 440 359

# APPLICATION OF THE DIFFRACTION MODEL TO AMORPHOUS MAGNESIUM ZINC ALLOYS

AD-A147 369

P. J. COTE  
L.V. MEISEL

OCTOBER 1984



US ARMY ARMAMENT RESEARCH AND DEVELOPMENT CENTER  
LARGE CALIBER WEAPON SYSTEMS LABORATORY  
BENET WEAPONS LABORATORY  
WATERVLIET N.Y. 12189

APPROVED FOR PUBLIC RELEASE; DISTRIBUTION UNLIMITED

DTIC FILE COPY

DTIC  
ELECTE  
OCT 31 1984  
S  
E

84 10 30 017

TABLE OF CONTENTS

	<u>Page</u>
INTRODUCTION	1
THEORETICAL MODELS	1
RESULTS AND DISCUSSION	3
CONCLUSIONS	6
REFERENCES	8

LIST OF ILLUSTRATIONS

1. Resistivity vs. temperature curves for 32.5% Zn composition.  
 $\Delta\rho = \rho(T) - \rho(300)$ ; no saturation. 5
2. Resistivity vs. temperature curves for 32.5% Zn composition.  
 $\Delta\rho = \rho(T) - \rho(300)$ ;  $q_D\Lambda = 11.6$  7

Accession For	
1005 GRAB	<input checked="" type="checkbox"/>
1005 103	<input type="checkbox"/>
1005 104	<input type="checkbox"/>
1005 105	<input type="checkbox"/>
1005 106	<input type="checkbox"/>
1005 107	<input type="checkbox"/>
1005 108	<input type="checkbox"/>
1005 109	<input type="checkbox"/>
1005 110	<input type="checkbox"/>
1005 111	<input type="checkbox"/>
1005 112	<input type="checkbox"/>
1005 113	<input type="checkbox"/>
1005 114	<input type="checkbox"/>
1005 115	<input type="checkbox"/>
1005 116	<input type="checkbox"/>
1005 117	<input type="checkbox"/>
1005 118	<input type="checkbox"/>
1005 119	<input type="checkbox"/>
1005 120	<input type="checkbox"/>
1005 121	<input type="checkbox"/>
1005 122	<input type="checkbox"/>
1005 123	<input type="checkbox"/>
1005 124	<input type="checkbox"/>
1005 125	<input type="checkbox"/>
1005 126	<input type="checkbox"/>
1005 127	<input type="checkbox"/>
1005 128	<input type="checkbox"/>
1005 129	<input type="checkbox"/>
1005 130	<input type="checkbox"/>
1005 131	<input type="checkbox"/>
1005 132	<input type="checkbox"/>
1005 133	<input type="checkbox"/>
1005 134	<input type="checkbox"/>
1005 135	<input type="checkbox"/>
1005 136	<input type="checkbox"/>
1005 137	<input type="checkbox"/>
1005 138	<input type="checkbox"/>
1005 139	<input type="checkbox"/>
1005 140	<input type="checkbox"/>
1005 141	<input type="checkbox"/>
1005 142	<input type="checkbox"/>
1005 143	<input type="checkbox"/>
1005 144	<input type="checkbox"/>
1005 145	<input type="checkbox"/>
1005 146	<input type="checkbox"/>
1005 147	<input type="checkbox"/>
1005 148	<input type="checkbox"/>
1005 149	<input type="checkbox"/>
1005 150	<input type="checkbox"/>



A-1

REPORT DOCUMENTATION PAGE		READ INSTRUCTIONS BEFORE COMPLETING FORM
1. REPORT NUMBER ARL CB-TR-84031	2. GOVT ACCESSION NO. A76-27269	3. RECIPIENT'S CATALOG NUMBER
4. TITLE (and Subtitle) APPLICATION OF THE DIFFRACTION MODEL TO AMORPHOUS MAGNESIUM ZINC ALLOYS		5. TYPE OF REPORT & PERIOD COVERED Final
		6. PERFORMING ORG. REPORT NUMBER
7. AUTHOR(s) P. J. Cote and L. V. Meisel		8. CONTRACT OR GRANT NUMBER(s)
9. PERFORMING ORGANIZATION NAME AND ADDRESS US Army Armament Research & Development Center Benet Weapons Laboratory, SMCAR-LCB-TL Watervliet, NY 12189		10. PROGRAM ELEMENT, PROJECT, TASK AREA & WORK UNIT NUMBERS AMCMS No. 6111.02.H600.011 Pron No. 1A325B541A1A
11. CONTROLLING OFFICE NAME AND ADDRESS US Army Armament Research & Development Center Large Caliber Weapon Systems Laboratory Dover, NJ 07801		12. REPORT DATE September 1984
		13. NUMBER OF PAGES 10
14. MONITORING AGENCY NAME & ADDRESS (if different from Controlling Office)		15. SECURITY CLASS. (of this report) Unclassified
		15a. DECLASSIFICATION/DOWNGRADING SCHEDULE
16. DISTRIBUTION STATEMENT (of this Report) Approved for Public Release; Distribution Unlimited		
17. DISTRIBUTION STATEMENT (of the abstract entered in Block 20, if different from Report)		
18. SUPPLEMENTARY NOTES		
19. KEY WORDS (Continue on reverse side if necessary and identify by block number) Amorphous Alloys Electron Transport Diffraction Model Saturation		
20. ABSTRACT (Continue on reverse side if necessary and identify by block number) Amorphous magnesium-zinc (a-MgZn) alloys comprise the best system available for testing the diffraction model for electron transport in non-crystalline alloys. They are simple metal binary alloys. Conventional methods exist for determining electronic parameters in the model. They exhibit low resistivities so that saturation effects are not expected to dominate. They are well characterized and extensive resistivity data are available. (CONT'D ON REFERSE)		

20. ABSTRACT (CONT'D)

Computed results presented here are based on a refinement of previous calculations; the alloy scattering matrix elements with computed phase shifts for Mg and Zn are used with the substitutional model instead of the adjusted effective potential assumed previously. Results obtained ignoring mean free path effects are in qualitative agreement with the data; agreement is surprisingly detailed when account is taken of saturation effects.

#### DISCLAIMER

The findings in this report are not to be construed as an official Department of the Army position unless so designated by other authorized documents.

The use of trade name(s) and/or manufacture(s) does not constitute an official indorsement or approval.

#### DISPOSITION

Destroy this report when it is no longer needed. Do not return it to the originator.

## INTRODUCTION

In a recent paper (ref 1) we presented quantitative results of diffraction model (ref 2) calculations of the temperature dependence of the resistivity of amorphous magnesium zinc (a-MgZn). The phase shift expansion of the scattering matrix elements as derived by Evans et al (ref 3) was used with the phase shifts adjusted to give the observed magnitude of the resistivity and to satisfy the Friedel sum rule. Saturation effects (ref 4) were included by invoking the Pippard-Ziman mean free path constraint (refs 1,2,5) on the electron-phonon interaction. A single effective scattering potential was used in place of the full alloy scattering matrix elements. Comparison of these computed results with the data of Matsuda and Mizutani (ref 6) in a-MgZn showed remarkable agreement between theory and experiment on all the many features of the temperature dependence of the resistivity. It was therefore considered worthwhile to refine the calculations by using the alloy scattering matrix elements with phase shifts computed for Mg and Zn in an extended version (ref 7) of the Ziman-Faber substitutional model (ref 8). Selected results pertaining to a-MgZn are presented here. Additional results relating to low resistivity alloys in general are given in Reference 9.

## THEORETICAL MODELS

We employ a form (ref 7) of the Ziman-Faber liquid alloy substitutional model (ref 8) which is appropriate for an amorphous Debye solid (ref 10). The result for the electrical resistivity is

$$\rho = \frac{12 \Omega_0}{e^2 h v_F^2} \int_0^1 d\left(\frac{K}{2k_F}\right) \left(\frac{K}{2k_F}\right)^3 |U(K)|^2 \quad (1)$$

---

References are listed at the end of this report.

where

$$|U(K)|^2 = c_1 c_2 |t_1(K) - t_2(K)|^2 I^\rho(K) + |c_1 t_1(K) + c_2 t_2(K)|^2 S^\rho(K) \quad (2)$$

and  $c_i$  and  $t_i(K)$  are the concentration and  $t$ -matrix for the  $i^{\text{th}}$  component.

The resistivity structure factor is given by

$$S^\rho(K) = e^{-2W(K)} a(K) + \frac{\alpha \theta_R}{T} \left(\frac{K}{2k_F}\right)^2 \int_0^1 d\left(\frac{q}{q_D}\right) \left(\frac{q}{q_D}\right)^2 n(x)(n(x)+1) F(q\Lambda) \int_0^1 \frac{d\Omega q}{4\pi} a(\bar{K}+q) \quad (3)$$

where  $\alpha = 3(2hk_F)^2 / Mk_B \theta_R$ .

The corresponding cross term integral is given as

$$I^\rho(K) = e^{-2W(K)} + \frac{\alpha \theta_R}{T} \left(\frac{K}{2k_F}\right)^2 \int_0^1 d\left(\frac{q}{q_D}\right) \left(\frac{q}{q_D}\right)^2 n(x)[n(x)+1] F(q\Lambda) \quad (4)$$

The partial geometric structure factors in the substitutional models are assumed to be identical and are given by

$$a(K) = \frac{1}{N} \sum_{m,n} \exp[iK \cdot (\vec{m} - \vec{n})] \quad (5)$$

where  $m$  and  $n$  represent the average ion positions.

The scattering matrix elements for the  $i^{\text{th}}$  component is given by

$$t_j(K) = \frac{2\pi h^3}{m(2mE_F)^{1/2} \Omega_0} \sum (2\ell+1) \sin \eta_{\ell}^j(E_F) P_{\ell}(\cos \theta) \quad (6)$$

where  $\eta_{\ell}^j(E_F)$  are the scattering phase shifts.

The Pippard-Ziman constraint (ref 5) on the electron-phonon interaction reflects the breakdown of the adiabatic approximation due to finite electron mean free paths  $\Lambda$  and is incorporated here through the Pippard function (ref 11)  $F(q\Lambda)$  where

$$F(y) = \frac{2}{\pi} \left[ \frac{y \tan^{-1} y}{y - \tan^{-1} y} - \frac{3}{y} \right] \quad (7)$$

In the long mean free path limit  $F(q\Lambda) \rightarrow 1$  and the above expressions reduce to standard diffraction model results.

The remaining terms in the above expressions have their usual meaning; other details and definitions are given in Reference 9.

## RESULTS AND DISCUSSION

The phase shifts for these calculations were obtained by constructing muffin tin potentials with the Mattheiss prescription (ref 12) using Herman and Skillman (ref 13) neutral atom wave functions. For Mg the Kmetko (ref 14) value of 0.75 of full Slater exchange was used. For Zn the value of 0.85 of full Slater exchange was used since this places the d-levels at approximately 9 eV below  $E_F$ , which is appropriate for Zn alloys. The phase shift values were then computed using modified versions of computer routines given by Loucks (ref 15). The  $\ell = 0$  to  $\ell = 3$  values at  $E_F$  in the 72 percent Mg alloy for Mg are -0.175, 0.085, 0.034, and 0.001, respectively. For Zn the corresponding values are 0.354, 0.294, -0.057, and 0.002.

The other parameters used in the computations were based on the following: x-ray data (ref 16) for a-Mg<sub>7</sub>Zn<sub>3</sub> show the main peak in the structure factor is located at  $k_p = 2.7 \text{ \AA}^{-1}$  for the a-MgZn composition range. We assume that  $k_p$  varies so that  $2k_F/k_p = 1.11$  is appropriate for the composition range; the average ionic mass was used for M; a Debye phonon spectrum is assumed and, since  $z \approx 2$ , we took  $q_D = k_F$ ; specific heat data (ref 17) give  $\theta_D = 295\text{K}$  for the low temperature limit, but we selected  $\theta_R =$

200K for the resistivity Debye temperature to fit the room temperature TCR. (For crystalline Mg,  $\theta_D = 390\text{K}$  and  $\theta_R = 340\text{K}$ , while for Zn,  $\theta_D = 310\text{K}$  and  $\theta_R = 175\text{K}$  (ref 18).) A geometric structure factor of Percus-Yevick form with packing fraction of 0.525 is appropriate for amorphous alloys (ref 18) and was used here.

Detailed experimental data for  $a\text{-Mg}_{1-x}\text{Zn}_x$  for  $.225 < x < .325$  were obtained by Matsuda and Mizutani (ref 6). All compositions show negative TCR's at the high temperatures and resistivity maxima ranging between 40 to 60K; most also show broad shallow minima centered at approximately 10K. Another feature found by Matsuda and Mizutani is that the resistivity varies as  $(T-T_M)^{3/2}$  for  $T > T_M$ , where  $T_M$  is the temperature at the resistivity maximum.

The results of the present calculation are shown in Figures 1 and 2. The computed magnitude of  $\rho$  is about  $40 \mu\Omega\text{cm}$ . In Figure 1 we see the  $\rho$  vs.  $T$  behavior computed from the standard diffraction model (Eqs. (1) through (7) with  $F(qA) = 1$ ): a maximum and a negative TCR at room temperature are obtained in the calculation, however,  $T_M$  is higher than observed by about a factor of two, the calculated magnitude of the TCR at room temperature is too small by at least a factor of four, and the size of the maximum is too large by two orders of magnitude. The low temperature  $T^2$  limit occurring in the standard diffraction model, (i.e.,  $\rho = \rho_0(1+BT^2)$  with  $B \cong 3 \times 10^{-6}\text{K}^{-2}$ ) holds up to about 15K. This is not consistent with the data either since the mean value for  $B$  obtained by Matsuda and Mizutani (ref 6) is  $0.5 \times 10^{-6}\text{K}^{-2}$  and the temperature range for this approximate quadratic dependence is considerably extended.

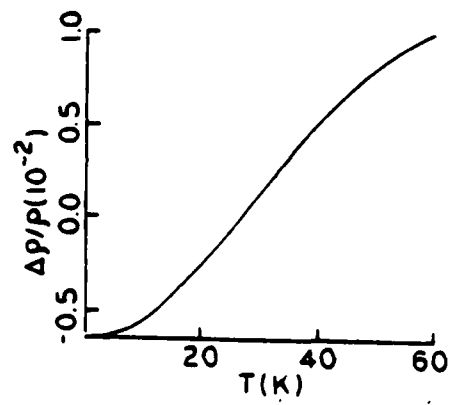
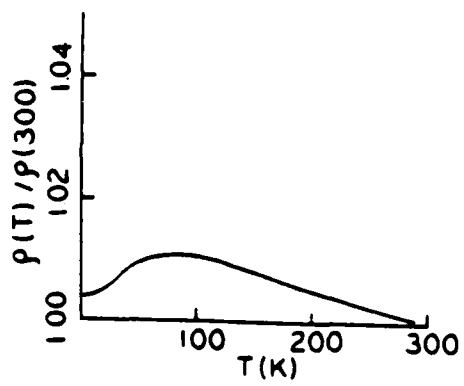


Figure 1. Resistivity vs. temperature curves for 32.5% Zn composition.  
 $\Delta\rho = \rho(T) - \rho(300)$ ; no saturation.

Figure 2 shows the result with saturation effects included. The value of  $q_D \Lambda$  was set at 11.6 to correspond to the observed  $\rho$  value at  $x = .325$  and to a saturation resistivity of  $200 \mu\Omega\text{cm}$ . The previous calculations (ref 1) with the effective potential approximation, including saturation, reproduced many of the observed features such as the presence of minima, the correct magnitude and approximate average position of the maxima, the  $(T-T_M)^{3/2}$  dependence, and the reduced magnitude of B. The present results show these features: for example, the value of B for  $x = .325$  is approximately  $0.5 \times 10^{-6} \text{K}^{-2}$  with an extended  $T^2$  range. In addition, the observed shape and position of the minima are obtained; the trends in size and position of the minimum and maximum in resistivity and the magnitude of the resistivity are also consistent with the data.

#### CONCLUSIONS

The results underscore the point that effects of finite electron mean free paths are important in the temperature dependence of the resistivity of amorphous alloys, even in alloys with resistivities as low as  $50 \mu\Omega\text{cm}$ . Only qualitative agreement with experiment is obtained if saturation is ignored. Earlier work (ref 2) showed that not even qualitative agreement with the diffraction model could be obtained at higher resistivities unless these effects are considered. The detailed agreement between the present computations, which include saturation, and the many features of the  $\rho$  vs. T data of a-MgZn is remarkable.

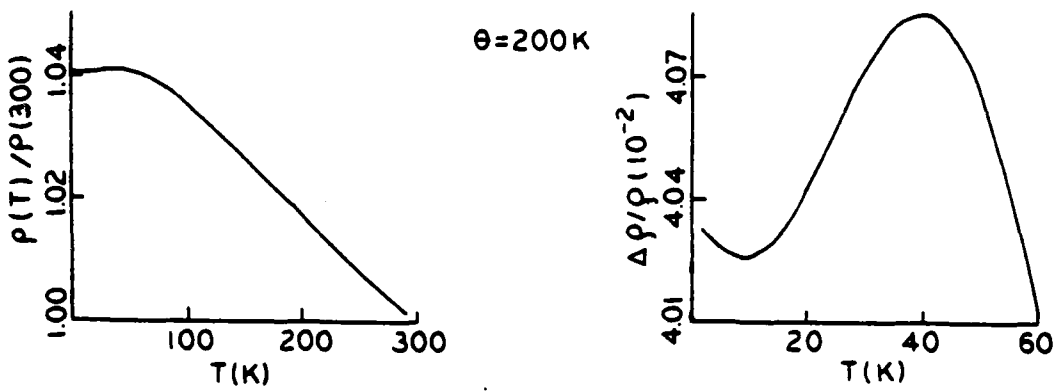


Figure 2. Resistivity vs. temperature for 32.5% Zn composition.  
 $\Delta\rho = \rho(T) - \rho(300)$ ;  $qD\lambda = 11.6$ .

## REFERENCES

1. L. V. Meisel and P. J. Cote, Phys. Rev. **B27**, 1983, p. 4617.
2. P. J. Cote and L. V. Meisel, "Electron Transport in Amorphous Metals," in: Topics in Applied Physics, (H.-J. Guntherodt and H. Beck, eds.), Vol. 46, Springer, Heidelberg, 1981, pp. 141-166; G. Baym, Phys. Rev. **A135**, 1964, p. 1691; J. M. Ziman, Phil. Mag. **6**, 1961, p. 1013; see also Reference 3.
3. R. Evans, B. L. Gyorffy, N. Szabo, and J. M. Ziman, "On the Resistivity of Liquid Transition Metals," in: The Properties of Liquid Metals, (S. Takeuchi, ed.), John Wiley and Sons, New York, 1973, p. 319.
4. See, for example, J. H. Mooij, Phys. Status Solidi **A17**, 1973, p. 521.
5. J. M. Ziman, Electrons and Phonons, Clarendon, Oxford, 1960, Chapter 5. See also P. J. Cote and L. V. Meisel, Phys. Rev. Lett. **40**, 1978, p. 1586.
6. T. Matsuda and U. Mizutani, J. Phys. **F12**, 1982, p. 1877.
7. P. J. Cote and L. V. Meisel, to be published.
8. T. E. Faber and J. M. Ziman, Philos. Mag. **11**, 1965, p. 153.
9. L. V. Meisel and P. J. Cote, "Electrical Resistivity in Low Resistivity Amorphous Alloys," U.S. ARDC Technical Report ARLCB-TR-84030, Benet Weapons Laboratory, Watervliet, NY, October 1984.
10. L. V. Meisel and P. J. Cote, Phys. Rev. **B16**, 1977, p. 2978.
11. A. B. Pippard, Philos. Mag. **46**, 1955, p. 1104.
12. L. F. Mattheiss, Phys. Rev. **A133**, 1964, p. 1399.
13. F. C. Herman and S. Skillman, Atomic Structure Calculations, Prentice Hall, Englewood Cliffs, NJ, 1963.

14. E. A. Kmetko, Phys. Rev. A1, 1970, p. 37.
15. T. L. Loucks, Augmented Plane Wave Method, Benjamin, New York, 1967.
16. T. Mizoguchi, N. Shiotani, U. Mizutani, T. Kudi, and S. Yamada, J. Phys. Paris, Colloq. 41, 1980, p. C8-183.
17. U. Mizutani and T. Mizoguchi, J. Phys F12, 1981, p. 1385.
18. G. T. Meaden, Electrical Resistance of Metals, Plenum Press, New York, 1965.
19. P. J. Cote, G. P. Capsimalis, and L. V. Meisel, Phys. Rev. B16, 1977, p. 4651.

TECHNICAL REPORT INTERNAL DISTRIBUTION LIST

	<u>NO. OF COPIES</u>
CHIEF, DEVELOPMENT ENGINEERING BRANCH	
ATTN: SMCAR-LCB-D	1
-DA	1
-DP	1
-DR	1
-DS (SYSTEMS)	1
-DS (ICAS GROUP)	1
-DC	1
CHIEF, ENGINEERING SUPPORT BRANCH	
ATTN: SMCAR-LCB-S	1
-SE	1
CHIEF, RESEARCH BRANCH	
ATTN: SMCAR-LCB-R	2
-R (ELLEN FOGARTY)	1
-RA	1
-RM	2
-RP	1
-RT	1
TECHNICAL LIBRARY	5
ATTN: SMCAR-LCB-TL	
TECHNICAL PUBLICATIONS & EDITING UNIT	2
ATTN: SMCAR-LCB-TL	
DIRECTOR, OPERATIONS DIRECTORATE	1
DIRECTOR, PROCUREMENT DIRECTORATE	1
DIRECTOR, PRODUCT ASSURANCE DIRECTORATE	1

NOTE: PLEASE NOTIFY DIRECTOR, BENET WEAPONS LABORATORY, ATTN: SMCAR-LCB-TL,  
OF ANY ADDRESS CHANGES.

TECHNICAL REPORT EXTERNAL DISTRIBUTION LIST

	<u>NO. OF COPIES</u>		<u>NO. OF COPIES</u>
ASST SEC OF THE ARMY RESEARCH & DEVELOPMENT ATTN: DEP FOR SCI & TECH THE PENTAGON WASHINGTON, D.C. 20315	1	COMMANDER US ARMY AMCCOM ATTN: SMCAR-ESP-L ROCK ISLAND, IL 61299	1
COMMANDER DEFENSE TECHNICAL INFO CENTER ATTN: DTIC-DDA CAMERON STATION ALEXANDRIA, VA 22314	12	COMMANDER ROCK ISLAND ARSENAL ATTN: SMCRI-ENM (MAT SCI DIV) ROCK ISLAND, IL 61299	1
COMMANDER US ARMY MAT DEV & READ COMD ATTN: DRUDE-SG 5001 EISENHOWER AVE ALEXANDRIA, VA 22333	1	DIRECTOR US ARMY INDUSTRIAL BASE ENG ACTV ATTN: DRXIB-M ROCK ISLAND, IL 61299	1
COMMANDER ARMAMENT RES & DEV CTR US ARMY AMCCOM ATTN: SMCAR-LC SMCAR-LCE SMCAR-LCM (BLDG 321) SMCAR-LCS SMCAR-LCU SMCAR-LCW SMCAR-SCM-O (PLASTICS TECH EVAL CTR, BLDG. 351N) SMCAR-TSS (STINFO) DOVER, NJ 07801	1 1 1 1 1 1 1 2	COMMANDER US ARMY TANK-AUTMV R&D COMD ATTN: TECH LIB - DRSTA-TSL WARREN, MI 48090	1
		COMMANDER US ARMY TANK-AUTMV COMD ATTN: DRSTA-RC WARREN, MI 48090	1
		COMMANDER US MILITARY ACADEMY ATTN: CHMN, MECH ENGR DEPT WEST POINT, NY 10996	1
		US ARMY MISSILE COMD REDSTONE SCIENTIFIC INFO CTR ATTN: DOCUMENTS SECT, BLDG. 4484 REDSTONE ARSENAL, AL 35898	2
DIRECTOR BALLISTICS RESEARCH LABORATORY ATTN: AMXBR-TSB-S (STINFO) ABERDEEN PROVING GROUND, MD 21005	1	COMMANDER US ARMY FGN SCIENCE & TECH CTR ATTN: DRXST-SD 220 7TH STREET, N.E. CHARLOTTESVILLE, VA 22901	1
MATERIEL SYSTEMS ANALYSIS ACTV ATTN: DRXSY-MP ABERDEEN PROVING GROUND, MD 21005	1		

NOTE: PLEASE NOTIFY COMMANDER, ARMAMENT RESEARCH AND DEVELOPMENT CENTER, US ARMY AMCCOM, ATTN: BENET WEAPONS LABORATORY, SMCAR-LCB-TL, WATERVLIET, NY 12189, OF ANY ADDRESS CHANGES.

TECHNICAL REPORT EXTERNAL DISTRIBUTION LIST (CONT'D)

	<u>NO. OF COPIES</u>		<u>NO. OF COPIES</u>
COMMANDER US ARMY MATERIALS & MECHANICS RESEARCH CENTER ATTN: TECH LIB - DRXMR-PL WATERTOWN, MA 01272	2	DIRECTOR US NAVAL RESEARCH LAB ATTN: DIR, MECH DIV CODE 26-27, (DOC LIB) WASHINGTON, D.C. 20375	1 1
COMMANDER US ARMY RESEARCH OFFICE ATTN: CHIEF, IPO P.O. BOX 12211 RESEARCH TRIANGLE PARK, NC 27709	1	COMMANDER AIR FORCE ARMAMENT LABORATORY ATTN: AFATL/DLJ AFATL/DLJG EGLIN AFB, FL 32542	1 1
COMMANDER US ARMY HARRY DIAMOND LAB ATTN: TECH LIB 2800 POWDER MILL ROAD ADELPHIA, MD 20783	1	METALS & CERAMICS INFO CTR BATTELLE COLUMBUS LAB 505 KING AVENUE COLUMBUS, OH 43201	1
COMMANDER NAVAL SURFACE WEAPONS CTR ATTN: TECHNICAL LIBRARY CODE X212 DAHLGREN, VA 22448	1		

NOTE: PLEASE NOTIFY COMMANDER, ARMAMENT RESEARCH AND DEVELOPMENT CENTER,  
US ARMY AMCCOM, ATTN: BENET WEAPONS LABORATORY, SMCAR-LCB-TL,  
WATERVLIET, NY 12189, OF ANY ADDRESS CHANGES.

END

FILMED

12-84

DTIC